AN EMBRYOLOGICAL STUDY OF FIVE SPECIES OF *BASSIA* ALL. (CHENOPODIACEAE)

GWENNETH J. HINDMARSH
Department of Botany, The University of New England

[Read 27th October, 1965]

Synopsis

Development of male and female gametophytes and embryogeny of *Bassia bicornis*, *B. brachyptera*, *B. divaricata*, *B. paradoxa* and *B. patenticuspis* is described.

Plate crystals of calcium oxalate were found in the perianth and ovary wall of all species, and anther filaments of some species.

The anther, which is tetrasporangiate, becomes four to five layered due to irregular divisions in the tapetum. Both amoeboid and secretory tapetum types occurred. Cytokinesis of the microspores is simultaneous and the mature pollen grain is three-celled.

The ovary contains a basal, campylotropous, bitegmic ovule which is crassinucellate. The hypodermal archesporial cell cuts off a parietal cell and the megaspore mother cell undergoes normal megasporogenesis. The chalazal megaspore of a linear tetrad develops into the monosporic eight-nucleate embryo sac of the *Polygonum* type.

Embryogeny conforms to the Chenopodiad type and the mature embryo is elongate and spiral. The endosperm is at first nuclear, but later becomes cellular and is digested by the developing embryo until only a cap remains over the tip of the radicle. In the seed the food storage region is the perisperm.

INTRODUCTION

Representatives of the family Chenopodiaceae are native to Australia in a wide variety of habitats, which include xerophytic and halophytic situations. In semi-arid areas, which are too dry for grasses, many genera such as *Atriplex*, *Bassia*, *Chenopodium*, *Kochia*, and *Rhagodia* are valuable fodder plants. The genus *Bassia*, according to Black (1948), consists of 60 species, of which about 50 are Australian endemics and the remainder occur in Europe and Asia. No indigenous members of the family have been studied embryologically and, although some overseas species of genera represented in Australia have been examined, no previous work of this nature has been carried out on *Bassia*.

MATERIALS AND METHODS

The material used in this investigation was collected in the field by Mr. E. Hoult in May, 1963, or from plants grown in the glasshouse from seeds collected in western New South Wales (Table 1).

Conventional paraffin sections were cut at 9–14 μ and stained with Delafield's Haematoxylin and Johansen's Safranin; supplementary examinations were made by dissections and squashes of fresh and preserved material.

The drawings, unless otherwise indicated, are of *B. paradoxa* and comparative studies were made with the other species.

MORPHOLOGY

Bassia paradoxa is a small shrub with narrow to linear, thick, alternate leaves which, together with the stems, bear a white woolly indumentum (Fig. 1). The hairs are multicellular and uniseriate (Figs 2, 3). The flowers, which are also hairy, are sessile, and 8–20 are united in each dense axillary cluster (Figs 4, 9), although according to Black (1948) clusters of 6–10 flowers are usual. Bisulputra (1960) has shown that the cluster is morphologically a condensed

dichasium. In the remaining species examined, the flowers occurred singly in the leaf axils due to the suppression of the lateral buds of the dichasium (Bisulputra, 1960). The development of the hairs, the perianth tube and the spines is variable (Figs 8–14) but is specifically distinct (Black, 1948).

The ovary is monocarpellary and unilocular with a solitary basal campylotropous ovule (Fig. 5). The elongated style terminates in two elongated stigmatic branches, although in some cases it is trifid due to the presence of

Table 1

List of species and locations from which material was collected

Species	Location	Collected from glasshouse
B. paradoxa (R. Br.) F. v. M.	31 m. W. Broken Hill	May '63—July '64
B. bicornis (Lindl.) F. v. M.	60 m. E. Quilpie, Q'ld.	May '63—Nov. '63
B. brachyptera (F. v. M.) R. H. Anderson	40 m. E. Broken Hill	—
B. divaricata (R. Br.) F. v. M.	70 m. N. Broken Hill	—
B. patenticuspis R. H. Anderson	—	Nov. '64—Feb. '65

a smaller third branch. Its surface is finely papillose and its open stylar canal communicates directly with the loculus (Fig. 6). The five stamens are obdiplostemonous with dorsifixed tetrasporangiate anthers and are at first enclosed within the perianth tube, but with elongation of the filament after maturity of the pollen grains they are displayed outside the woolly mat of hairs surrounding the flowers (Fig. 7). Introrse dehiscence occurs by means of longitudinal slits.

Table 2

Figures in microns indicate the average length of the larger crystals

Species	Top of ovary	Base of ovary	Perianth	Anther
B. paradoxa	20	5	9	—
B. bicornis	25	15	15	15
B. divaricata	12	4	10	4
B. brachyptera	14	13	11	8
B. patenticuspis	17	20	17	—

Crystals

Plate crystals were present in the perianth and ovary wall of all species studied (Figs 15, 16) and were identified as calcium oxalate by their solubility in 2N hydrochloric acid and their insolubility in 20% acetic acid. Although their shape was constant they varied in length from 2 to 30 μ, the average size for the larger ones varying between species and according to their location within the flowers (Table 2). The larger crystals were solitary and almost completely filled the cells, while in other instances there were up to four smaller ones present (Figs 17, 18). In *B. bicornis*, and to a lesser extent in the other species, the crystal-containing cells were larger than those lacking them (Figs

Figs 1–8. Morphology of *B. paradoxa*. 1, 4, 7, 8, Flower clusters of different ages; 2, 3, Hairs; 5, The gynoecium; 6, Stylar canal.
Figs 9–14. Fruits: 9, *B. paradoxa*; 10, 11, *B. patenticuspis*; 12, *B. bicornis*; 13, *B. divaricata*; 14, *B. brachyptera*.
Figs 3, 4, 6–8, 11, 12, in L.S.; remainder whole mounts.
(*c*, crystals; *pg*, pollen grains; *vs*, vascular strand.)
Figs 1, 7, ×3; 2, 3, ×220; 4, 9–14, ×7; 5, ×30; 6, ×130; 8, ×13.

17, 19). In the course of floral development, the crystals were first observed when the ovule was at the megaspore mother stage. They appeared in the inner hypodermal layer of the perianth lobes and tube, connecting with a broad crystal-bearing layer at the base of the ovary. Similarly, crystals were deposited in the upper hypodermal cells of the inner wall of the ovary wall and followed up the hollow style but with reduced size and frequency. A relationship was noted in the ovary between the absence of the crystals in the hypodermis and the radial elongation of the overlying inner epidermal cells (Figs 20, 21), while cells above and below these areas, which contained crystals in the hypodermis, were smaller although still glandular in appearance (Fig. 22). By the time of anthesis, the crystal layers had become thickened through further deposition of crystals in the second to the fourth sub-hypodermal cell layers where they persisted into the fruiting stage.

In *B. bicornis*, *B. brachyptera*, and *B. divaricata* a small number of crystals were also found in the central cells of some anther filaments but their distribution followed no definite pattern.

The Microsporangium

The undifferentiated anther is at first ovoid in cross section, but becomes rectangular due to radial expansion resulting from localized cell divisions. The cells are initially of similar size and non-vacuolate with prominent nuclei, after which four hypodermal, uniseriate rows differentiate as archesporial cells (Figs 23, 24), and initiate the formation of the four sporangia.

(*a*) *Wall Formation*

Each archesporial cell divides periclinally to form an inner primary sporogenous cell and an outer parietal cell which undergoes anticlinal divisions and, together with the adjacent cells from the ground tissue, forms the primary parietal layer, which encloses the sporogenous tissue (Figs 25, 26). Periclinal division of the primary parietal layer forms the secondary parietal layer and the outer endothecial layer (Figs 27, 28), whose cells divide only anticlinally. A periclinal division of the secondary parietal layer then gives rise to a single middle layer and to the tapetum, which may become irregularly two-layered due to further periclinal cell divisions (Figs 29–31). At this stage the microsporangium wall consists of four or five layers, the epidermis, the endothecium, the middle layer, and the tapetum which may be irregularly two-layered. The development of the wall layers is the same as that outlined diagrammatically in *Themeda australis* (Woodland, 1964, Fig. 7).

A four-layered wall is the usual condition in members of the Chenopodiaceae ; however, in *Beta vulgaris* (Artschwager, 1947) more than four layers have been described while, according to Miller, Kline and Weber (1959), in *Chenopodium ambrosioides* either one or two middle layers are present.

The pressure exerted by the expanding sporogenous tissue stretches all the wall layers tangentially and, although some anticlinal divisions occur, these cease when vacuolation sets in prior to the differentiation of the wall layers.

After the initial stretching of the tapetal cells rapid cytoplasmic synthesis occurs, and the cells increase in size and become glandular in appearance, with prominent nuclei and dense cytoplasm. When the adjacent microspore mother cells enter Prophase I many of the tapetal nuclei undergo an apparently normal mitotic division, in which the spindles are obliquely orientated within the cells (Figs 32, 33), and the cells become binucleate (Fig. 34), although fusion may occur and result in the formation of a single large polyploid nucleus (Fig. 35).

The tapetal cells first show signs of breakdown just prior to the release of the microspores from the tetrads (Fig. 36). This is indicated by the contraction of the protoplasm, which is followed by disorganization of the bounding

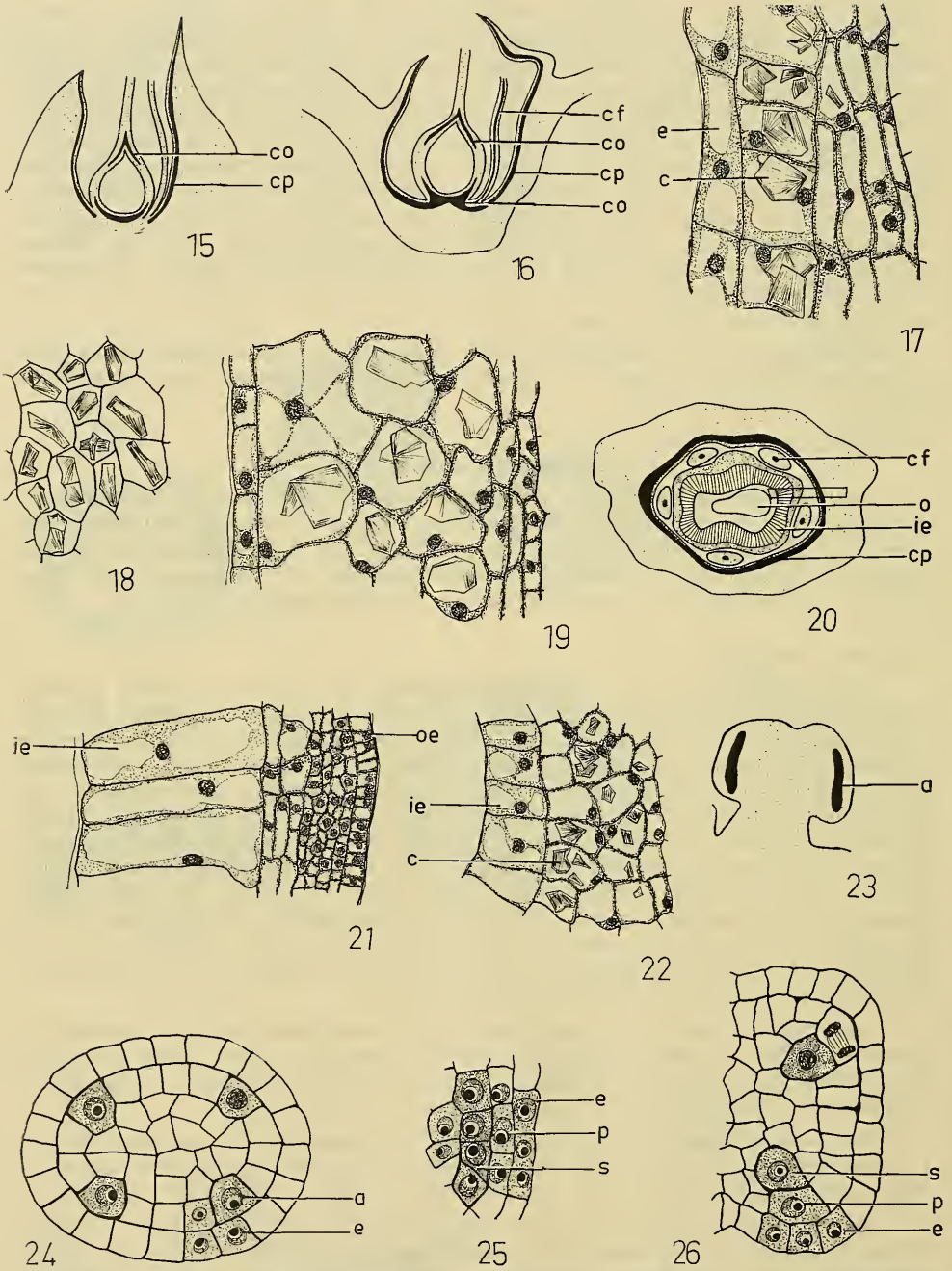

Figs 15–22. Calcium oxalate crystals. 15, Distribution of crystals in *B. paradoxa*; 16, Distribution of crystals in *B. divaricata*; 17, L.S. of *B. paradoxa* perianth; 18, *B. patenticuspis*, surface view of perianth crystals; 19–22, *B. bicornis*: 19, L.S. of perianth; 20, T.S. of flower; 21, Ovary wall as in Fig. 20; 22, T.S. of wall at top of the ovary.

Figs 23–26. Development of the microsporangium. Figs 23, 25 in L.S. (*a*, archesporium; *c*, crystals; *cf*, crystals in the anther filament; *co*, crystals in the ovary wall; *cp*, crystals in the perianth; *e*, epidermis; *ie*, inner epidermis of ovary wall; *o*, ovary; *oe*, outer epidermis of the ovary wall; *p*, primary parietal layer; *s*, sporogenous tissue.)
Figs 15, 16, 20, ×20; 17, ×320; 18, 19, 24–26, ×540; 21, 22, ×220; 23, ×130.

membrane (Fig. 37). At a later stage, when the pollen grains enter the ' signet ring ' configuration, it is usual in *B. paradoxa* for the inner walls of the tapetal cells to degenerate and so allow the protoplasts to form a continuous mass around the periphery of the loculus. As a result, the pollen grains come into contact with, and lie between, the remaining portions of the tapetal cells (Fig. 38). At this point, the nuclei show signs of degeneration but maintain their identity as dense areas in the tapetal cytoplasm until it is absorbed. Finally, the tapetum is represented by small oval globules on the inner walls of the endothecium (Fig. 39), which disappear before dehiscence (Fig. 44). In *B. brachyptera*, *B. divaricata*, *B. patenticuspis*, as well as *B. paradoxa*, the contents of the tapetal cells break down and are absorbed *in situ*; the tapetum conforms to the secretory or glandular type. In some anthers of *B. paradoxa*, however, after dissolution of the cell walls, the protoplasts become amoeboid and move into the loculus between the recently liberated tapetal microspores, forming a periplasmodium (Fig. 43). The liberated tapetal nuclei maintained their identity, and underwent mitotic divisions, indicating that this was a ' true '

TABLE 3

Types of tapetum in the species of Bassia *studied*

	Secretory	Amoeboid	
		Periplasmodium	No Periplasmodium
B. paradoxa	+	+	+
B. bicornis	—	—	+
B. brachyptera	+	—	—
B. divaricata	+	—	—
B. patenticuspis	+	—	—

periplasmodium, although in some sections of *B. paradoxa* the tapetal cells appeared to become detached and lie between the developing pollen grains, forming an apparently ' false ' periplasmodium (Fig. 40). However, on examination of serial sections it was seen that these cells were still in contact with the endothecium, and the pollen grains were merely lodged between the degenerating cells of the glandular tapetum (Fig. 38). An additional variation in *B. bicornis*, and of occasional occurrence in *B. paradoxa*, is the formation of an amoeboid tapetum which does not form a periplasmodium (Table 3). The protoplasts, which maintain their contact with the endothecium, become enlarged and vacuolated, and protrude into the loculus between the developing pollen grains, where they are absorbed (Fig. 41).

The occurrence of both a secretory and an amoeboid tapetum in the same species is unusual and, in some instances in *B. paradoxa*, both types were found in sporangia of adjacent anthers within the same flower, with a higher proportion of aborting microspores being found in the loculi with a secretory tapetum (Figs 42, 43). The only previous record in which both tapetal types occur is in the male-sterile plants of *Beta vulgaris* (Artschwager, 1947) where the periplasmodium is thought to delay pollen abortion, since in those microsporangia with a secretory tapetum the microspores degenerate while still retained in the tetrads. In fully fertile flowers of the same species Artschwager (1927) had previously reported only a secretory tapetum. In the present investigation, about 60% of microspores were degenerating in microsporangia with a secretory tapetum (Fig. 42), as against only about 10% in those with an amoeboid tapetum (Fig. 43).

Variation of tapetal behaviour is common within the family and, according to Mahabale and Solanky (1954*a*) in *Arthrocnemum indicum*, although it is of

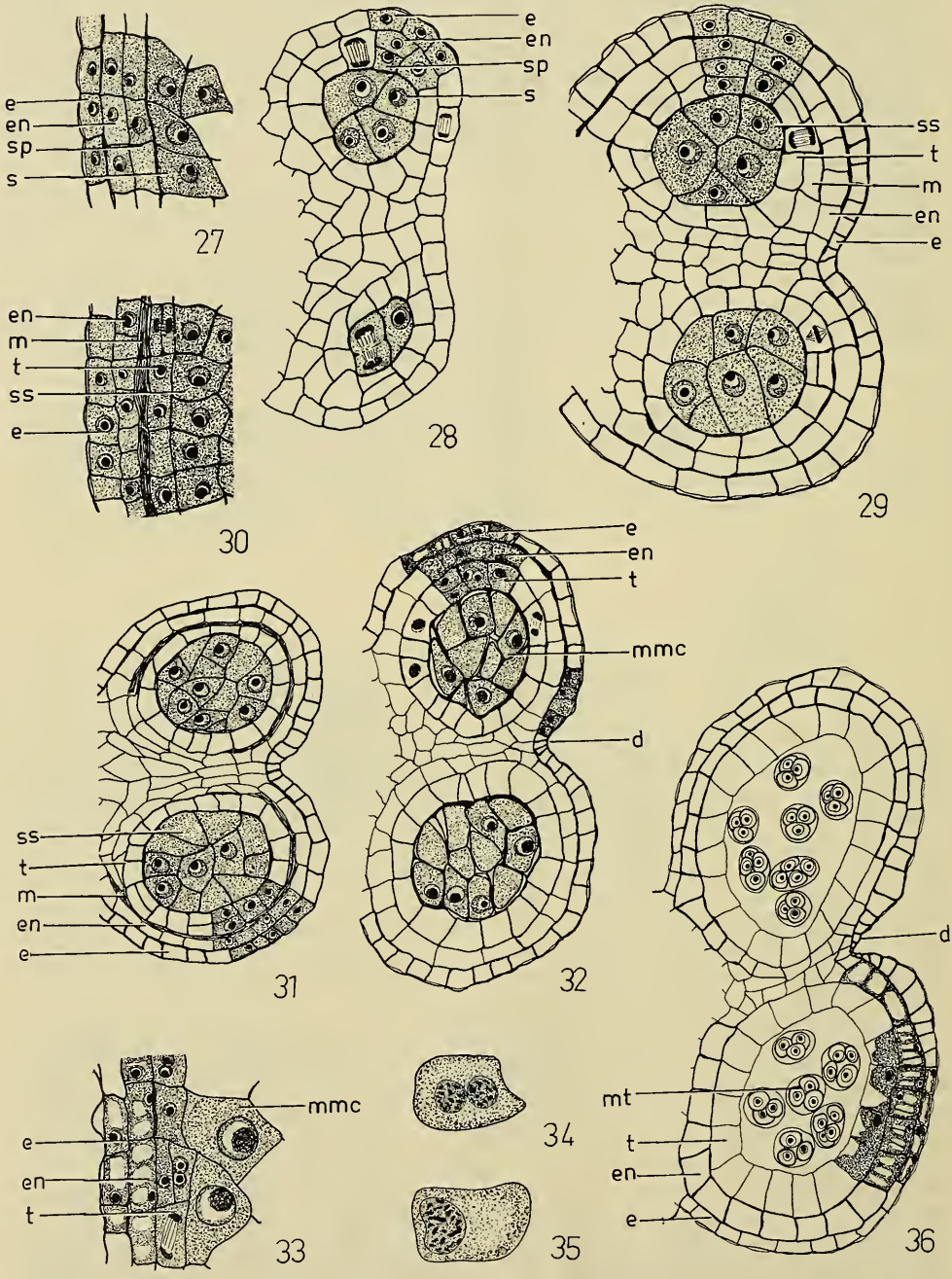

Figs 27–36. Development of the microsporangium. Figs 27, 30, 33, in L.S., remainder in T.S. Figs 34, 35, Tapetal cells.

(*d*, region of dehiscence ; *e*, epidermis ; *en*, endothecium ; *m*, middle layer ; *mmc*, microspore mother cell ; *mt*, microspore tetrad ; *s*, sporogenous tissue ; *sp*, secondary parietal layer ; *ss*, secondary sporogenous tissue ; *t*, tapetum.)

Figs 27–30. ×540 ; 31, 32, 36, ×310 ; 34, 35, ×780.

the secretory type, the " walls of the tapetal cells break down and the protoplasts coalesce to form a continuous mass at the periphery of the pollen chamber " which is similar to that reported in *Chenopodium ambrosioides* (Mahabale and Solanky, 1954*b*), *Kochia scoparia* (Mahabale and Solanky, 1953*b*) and *Suaeda fruticosa* (Mahabale and Solanky, 1953*a*). In *Chenopodium album* (Bhargava, 1936), however, although the tapetum is amoeboid it does not form a periplasmodium, and a similar condition is indicated by the illustration of Mahabale and Solanky (1954*c*) in *Chenopodium murale*, although the authors state that a periplasmodium forms.

The middle layer shows signs of stretching and of being crushed when the microspore mother cells are formed (Figs 31, 32), and at the microspore tetrad no remains are visible (Fig. 36).

The endothecial cells contain many starch grains (Fig. 45) which disappear after microsporogenesis, and the cells then become vacuolated, followed by the deposition of dimorphic ' fibrous ' wall thickenings. The cells from the connective region to about a third way around each sporangium are thickened in a scalariform manner (Fig. 46), while those extending to near the region of dehiscence bear numerous ' fibrous ' rods which are united at their bases and extend out along the tangential wall (Figs 47, 48). The first six or seven cells on either side of the point of dehiscence do not bear any thickenings and become highly vacuolated before breaking down completely at dehiscence (Fig. 40).

The epidermal cells become vacuolated simultaneously with the rounding off of the microspore mother cells prior to meiosis (Fig. 33), and all except those external to the ' non-fibrous ' cells of the endothecium are greatly stretched tangentially. At dehiscence they form a dead layer of cells over the endothecium, while those in the region of dehiscence increase in size at the same time as the thickenings are laid down in the endothecium (Fig. 48).

Introrse dehiscence takes place by a longitudinal slit in each side of the anther at the junction of the outer wall and the intersporangial septum (Figs 48, 49).

(*b*) *Microsporogenesis and Male Gametogenesis*

The primary sporogenous cells undergo two transverse and one vertical division to form the secondary sporogenous cells which then divide obliquely to form the microspore mother cells (Fig. 32), which round off and enter meiosis (Figs 50–52) followed by simultaneous cytokinesis. The occurrence of secondary spindles is common at telophase II (Figs 53, 54). The microspore tetrads are tetrahedral and isobilateral (Figs 56, 57), but in *B. bicornis* some decussate tetrads were found (Fig. 55). Separation of the microspores is accomplished by centripetal furrows and they are at first angular when liberated by the gelatinization of the enclosing wall of the microspore mother cell (Figs 58, 59). The appearance of a vacuole in the dense cytoplasm represents germination into the one-nucleate pollen grain or male gametophyte, and as this vacuole increases in size the nucleus becomes displaced laterally and the pollen grain assumes the ' signet ring ' configuration (Fig. 61).

Cytoplasmic synthesis reduces, and finally obliterates, the vacuole, and nuclear division is followed by the formation of the small generative cell (Figs 62, 63), which undergoes a further division to form the two male gametes (Figs 64, 65). It is in this three-celled condition that the pollen grain is shed. The deposition of exine is first apparent after the microspores are released from the tetrad and it thickens irregularly as the pollen grain increases in size to give the granular appearance of the mature polyforate pollen grain (Fig. 41).

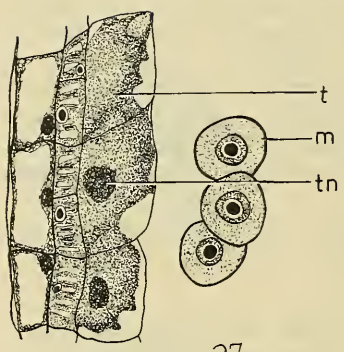

37

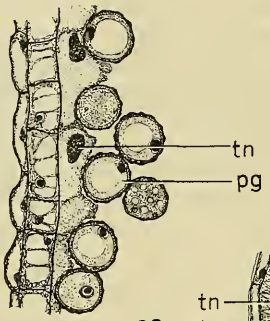

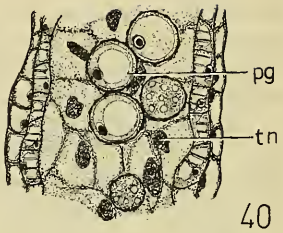

40

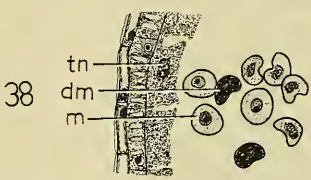

38

42

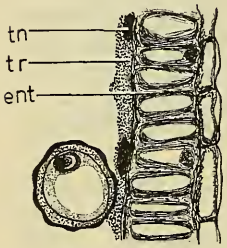

39

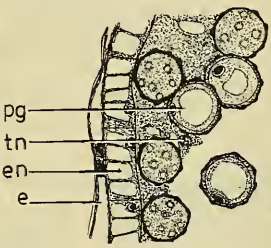

41

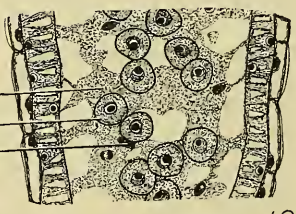

43

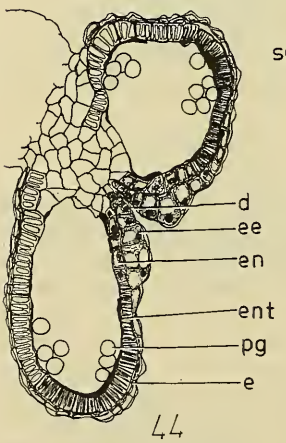

44

45

46

47

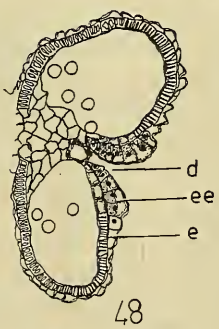

48

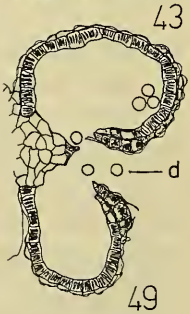

49

50

51

52

53

54

55

56

57

58

59

60

61

62

63

64

65

The Megasporangium

(*a*) *Development of the Ovule*

The primordium of the ovule develops at the base of the ovary when the microsporangium wall is two-layered, and two integumentary primordia appear as folds at the base of the nucellus simultaneously with the differentiation of the archesporial cell (Figs 66, 67). The integuments are at first two-layered, but further cell divisions occur in the inner integument and extend it beyond the slower growing outer one which has no part in the formation of the micropyle (Figs 69, 84). This form of integumentary development is commonly found in this family. A prominent air space was observed in the chalazal region between the integuments. During the differential growth of the ovule, which assumes a campylotropous form, the funiculus becomes elongated and results in the micropylar end of the ovule coming to lie across the base of the funiculus (Figs 68–70). A single vascular strand of annular and spiral vessels differentiates in the funiculus and passes to the chalazal region of the ovule (Fig. 84).

(*b*) *Megasporogenesis*

A single hypodermal archesporial cell makes its appearance at the apex of the ovule (Fig. 71) and divides periclinally to form an outer primary parietal cell and a megaspore mother cell, which is consistent with other records for this family. Mahabale and Solanky (1954*a*) quote Billings (1934) as having reported parietal cell formation in the ovule of *Atriplex hymenelytra* and, while this may well be true, it should be pointed out that Billings' statement referred to the behaviour of the anther archesporium. The parietal cell divides both anticlinally and periclinally and, together with similar divisions in the overlying nucellar epidermis, forms the massive nucellus of the crassinucellate ovule (Figs 72–74).

The megaspore mother cell undergoes meiosis accompanied by cytokinesis and gives rise to a dyad followed by a linear tetrad of megaspores (Figs 73, 74). In the Chenopodiaceae, the chalazal megaspore is invariably functional and, with vacuolation, increases in size at the expense of the three non-functional megaspores until it occupies the place which was filled previously by the tetrad (Figs 75, 76).

(*c*) *Female Gametogenesis*

The one-nucleate embryo sac is embedded deeply within the nucellus and, following nuclear division, passes into the two-nucleate stage in which the nuclei are separated by a central vacuole (Fig. 77). Both nuclei then divide simultaneously to form a four-nucleate embryo sac in which the central vacuole is retained (Fig. 78), and a third post-meiotic mitosis gives rise to an unorganized, eight-nucleate embryo sac in which small vacuoles separate the nuclei (Fig. 79). Cytokinesis follows rapidly to form seven cells, of which the central endosperm cell is binucleate (Fig. 80). In its development, the embryo sac is, therefore, of the monosporic, *Polygonum* or 'normal' type which has been reported in all other species investigated in this family.

Legends to figures on opposite page.

Figs 37–43. Types of tapetum. 37–39, Secretory tapetum; 40, 'False' periplasmodium; 41, *B. bicornis*—amoeboid tapetum, but no periplasmodium forms; 42, Secretory tapetum with degenerating microspores; 43, Periplasmodium.

Figs 44–49. Maturation of the anther wall and dehiscence; 45, Endothecial cell; 46, Scalariform thickening; 47, Rod thickening.

Figs 50–65. Formation of the microspores and the male gametes.
(*d*, region of dehiscence; *dm*, degenerating microspores; *e*, epidermis; *ee*, enlarged epidermal cells; *en*, endothecium; *ent*, endothecium with thickenings; *g*, germ pore; *gc*, generative cell; *m*, microspores; *mg*, male gametes; *p*, periplasmodium; *pg*, pollen grains; *sg*, starch grains; *t*, tapetum; *tn*, tapetal nuclei; *tr*, tapetal remains; *vc*, vegetative cell.)
Figs 37, ×780; 38, 40–43, ×320; 39, ×540; 44, ×90; 45–47, 50–65. ×360; 48, 49, ×53.

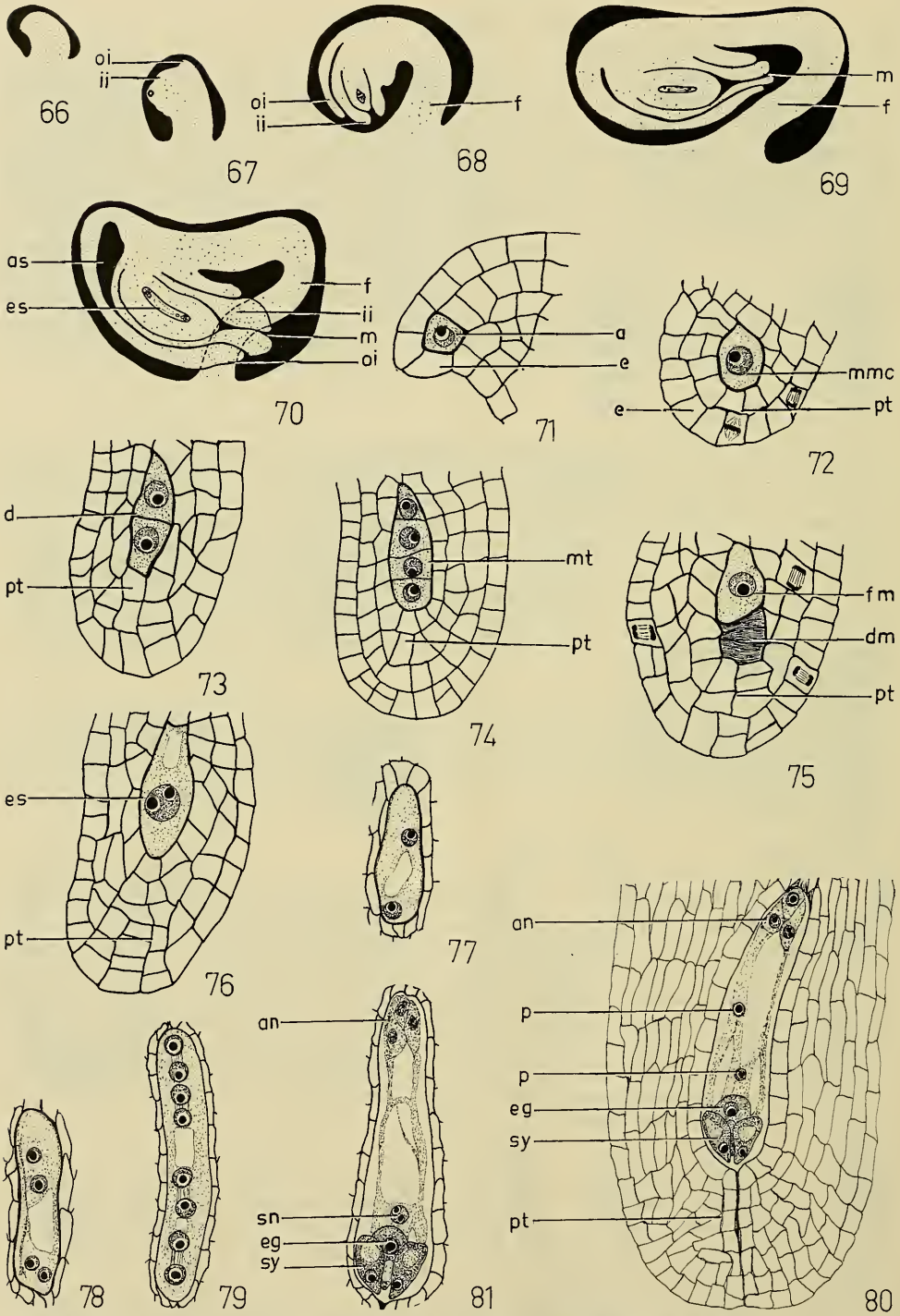

Figs 66–70. Development of the ovule. Figs 71–81. Megasporogenesis and embryo sac development.
(*a*, archesporium ; *an*, antipodals ; *as*, air space ; *d*, dyad ; *dm*, degenerating megaspores ; *e*, epidermis ; *eg*, egg ; *es*, embryo sac ; *f*, funiculus ; *fm*, functional megaspore ; *ii*, inner integument ; *m*, micropyle ; *mmc*, megaspore mother cell ; *mt*, megaspore tetrad ; *oi*, outer integument ; *pt*, parietal tissue ; *sn*, secondary nucleus : *sy*, synergids.)
Figs 66–70, ×80 ; 71–81, ×540.

The three antipodal cells are short lived and do not persist after fertilization. The binucleate endosperm cell consists of the original central vacuole surrounded by a thin layer of cytoplasm containing the polar nuclei. Just before fertilization, the chalazal polar nucleus migrates to the micropylar pole of the cell, where it becomes closely associated and then fuses with the micropylar polar nucleus to form the secondary nucleus (Figs 80, 81). The remaining three nuclei of the embryo sac form the egg apparatus which consists of two synergids and the egg (Fig. 80). The synergids, which are situated below the micropyle, are wedge-shaped, and their nuclei are apically situated, while a large vacuole occupies the base of each cell. The synergids commence degeneration as the pollen tube makes its way into the embryo sac, but their remains are still visible at the two-celled stage of the pro-embryo (Fig. 83). The egg cell is overlaid by the synergids and is at first non-vacuolate, but a large vacuole forms in the micropylar region of the cell at maturity.

The mature embryo sac becomes elongated in its chalazal region and it is enclosed by the persisting parietal and nucellar tissues (Fig. 81).

Fertilization

Large numbers of germinating pollen grains were found on the stigma (Fig. 5) and, although they were monosiphonous, branching frequently occurred on the stigmatic papillae to give the appearance of bisiphonous grains (Fig. 82). The pollen tubes grow down the surface of the papillae and between the loosely-packed cells of the stigmatic branches, finally reaching the hollow stylar canal which is in direct communication with the loculus of the ovary. At the base of the stylar canal, the pollen tubes encounter the funiculus of the ovule which is in contact with the upper wall of the ovary, and follow its course to the micropyle (Fig. 83). In some instances pollen tubes passed directly from the stylar canal to the outer integument and then to the micropyle over the surface of the integuments, thereby passing the funiculus and taking, apparently, a longer route. After penetrating the micropyle, the pollen tube makes its way between the elongated cells of the nucellus which encloses the embryo sac and, although more than one pollen tube reaches the ovule, each branching freely and becoming entangled with each other, only one appears to liberate male gametes and effect double fertilization. The pollen tubes do not persist into embryogeny.

Post-fertilization Changes

(*a*) *Endosperm*

Division of the primary endosperm nucleus precedes that of the zygote and is not accompanied by wall formation, so that the endosperm is of the nuclear type (Fig. 84). After further divisions, the free nuclei are distributed around the proembryo and the periphery of the embryo sac in cytoplasmic strands in which starch grains are also visible (Fig. 85). Nuclear divisions continue until the embryo sac is almost filled with endosperm (Fig. 86), and cell formation is initiated in the micropylar region when the embryo has become spherical (Fig. 87). Wall formation proceeds slowly and free nuclei are still visible in the chalazal region until after the initiation of the cotyledons (Figs 88, 89). The embryo digests the endosperm as it increases in size and finally only a small cap remains over the apex of the radicle (Fig. 90).

(*b*) *Embryogeny*

The zygote enlarges but does not divide until after several free endosperm nuclei have formed (Figs 84, 91). A transverse division forms the two-celled proembryos, or first cell generation, which consists of an upper cell, *ca*, and a basal cell, *cb* (Figs 85, 92). These cells divide simultaneously forming the superposed cells *l*, *l'*, *m*, and *ci* of the second cell generation (Fig. 93). Each

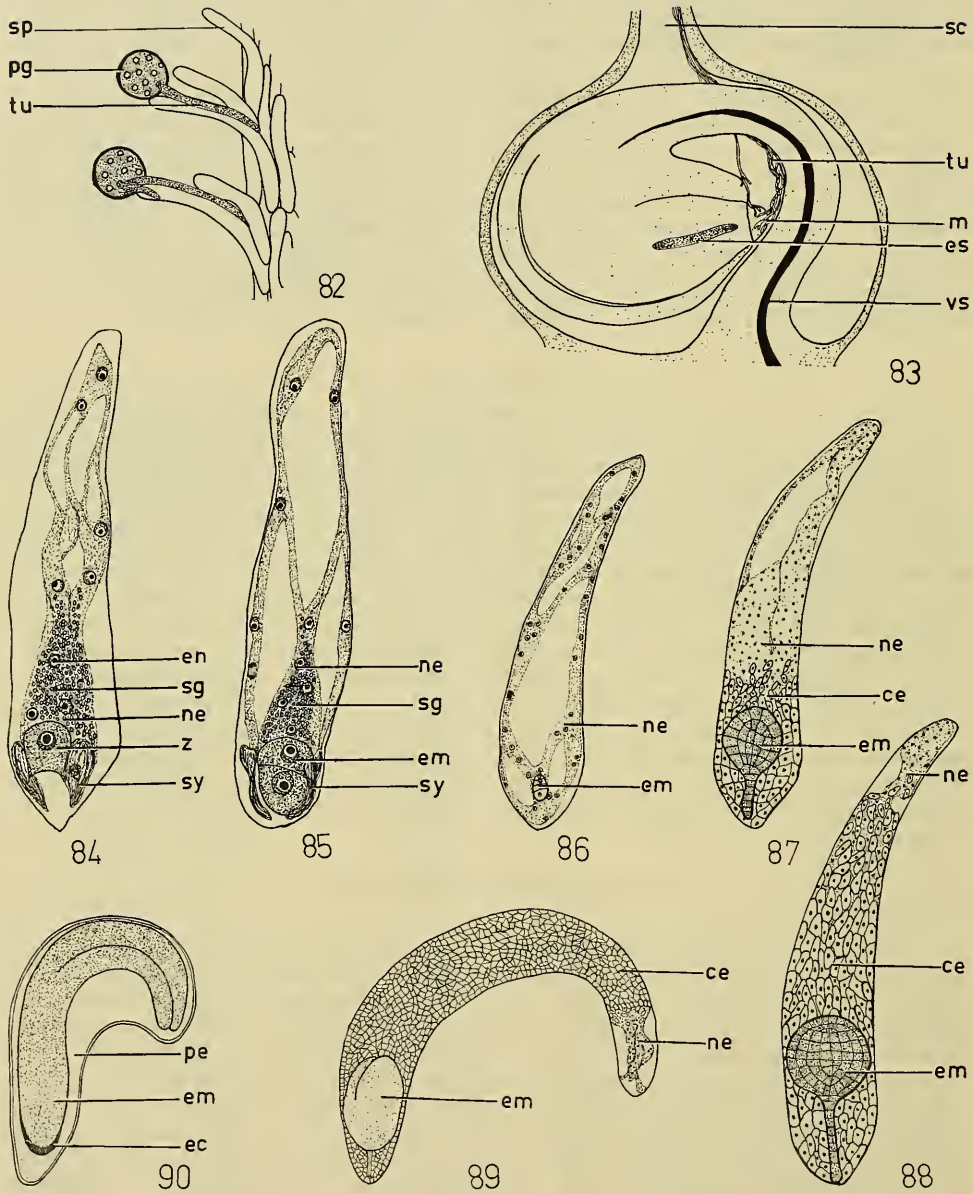

Figs 82, 83. Growth of the pollen tubes, drawn from whole mounts. Figs 84–90. Endosperm development.

(*ce*, cellular endosperm ; *ec*, endosperm cap ; *em*, embryo ; *en*, endosperm nuclei ; *es*, embryo sac ; *ne*, nuclear endosperm ; *pe*, perisperm ; *pg*, pollen grains ; *sc*, stylar canal ; *sg*, starch grains ; *sp*, stigmatic papilla ; *sy*, synergids ; *tu*, pollen tubes ; *vs*, vascular strand ; *z*, zygote.)

Figs 82, ×220 ; 83, 86–88, ×130 ; 84, 85, ×540 ; 89, ×50 ; 90, ×20.

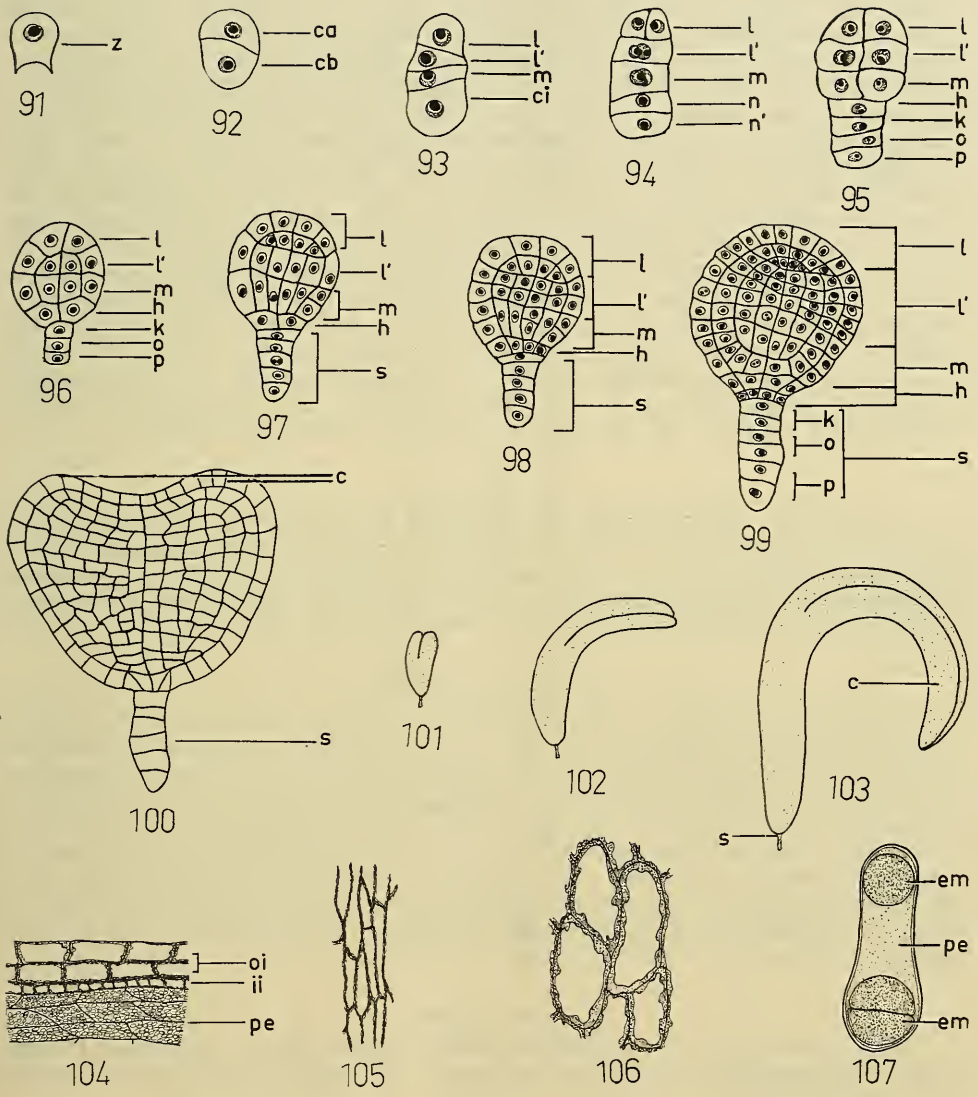

Figs 91–107 : 91–103, Embryogeny and changes in shape and dimensions of the embryo ; 104–107, The mature seed ; 104, T.S. of seed wall ; 105, Tangential section of cells of the inner integument ; 106, Tangential section of cells of the outer integument ; 107, T.S. of seed. Lettering of the embryo follows the system of Soueges.

(*c*, cotyledon ; *em*, embryo ; *ii*, inner integument ; *oi*, outer integument ; *pe*, perisperm ; *s*, suspensor ; *z*, zygote.)

Figs 96–100, ×220 ; 101–103, 107, ×20 ; 104–106, ×330.

of these divides to give the eight-celled proembryo of the third cell generation, the lowest cell, *ci*, dividing transversely into *n* and *n'*, while the other three cells divide vertically (Fig. 94). In the fourth cell generation *n* and *n'* both undergo a transverse division to give rise to *h*, *k*, *o*, and *p* (Fig. 95), which is followed by quadrants being produced in tiers *m* and *l'* and, at a later stage, *l* (Fig. 96). The embryo proper develops from *l*, *l'*, *m*, and *h*, while *k*, *o*, and *p* form the uniseriate suspensor which is elongate and usually consists of six superposed cells, which results from further divisions in these cells (Fig. 98). However, in *B. patenticuspis* further divisions may form eight superposed cells. The cells of the suspensor when fully formed are vacuolate and the basal one enlarges slightly, remaining in contact with the nucellus (Figs 87, 99). The hypophysis cell, *h*, divides vertically into two juxtaposed cells (Fig. 96), and a similar division follows in the inner cells, and a transverse division in the outer cells of the tiers *l*, *l'*, and *m* (Fig. 97). The cells of tier *h* divide longitudinally to form the hypophyseal quadrant, which then divides horizontally (Figs 98, 99). The embryo proper is now spherical in form due to the enlargement of cells in tiers *l*, *l'*, and *m*. After further divisions, the embryo becomes heart-shaped and the primordia of the cotyledons differentiate (Fig. 100). The embryo sac meanwhile has continued its growth into the chalazal region of the ovule, becoming spirally curved to accommodate the enlarging embryo which, at maturity, is elongate and spiral (Figs 101–103). This type of embryo development conforms to the Chenopodiad type of Soueges (1920).

Polyembryony

No case of polyembryony was observed in the species investigated, but Cole (1895) reported this to be the normal condition in *Beta rubra*, in which a single seed produced as many as four plants. Favorsky (1928) also described polyembryony resulting from nucellar budding in *Beta vulgaria*, but Artschwager and Starrett (1933) reported that it did not occur in their material.

The Mature Seed

The fully developed integuments are two-layered except in the micropylar region where they are four to six cell layers in thickness. During development the cells of the outer layer of the inner integument gradually lose their contents and disappear, while the inner layer remains intact into the seed stage (Figs 104, 105). Both the cell layers of the outer integument persist and deposition of tannin occurs in their cells, while small areas of thickening develop on the tangential walls of the outer cells and project into the lumina (Figs 104, 106). As the endosperm is digested, starch grains are deposited in the nucellus so that in the mature seed the food storage region is the perisperm (Figs 90, 107), which is characteristic of the Centrospermales.

Acknowledgements

The author wishes to express her thanks to members of the Botany Department and especially to Associate Professor G. L. Davis for her guidance during this investigation.

References

Artschwager, E., 1947.—Pollen degeneration in male sterile sugar beets, with special reference to the tapetal plasmodium. *J. Agric. Res.*, 75 : 191–197.

———, and Starrett, R. C., 1933.—The time factor in fertilization and embryo development in the sugar beet. *J. Agric. Res.*, 47 : 823–843.

Bhargava, H. R., 1936.—The life history of *Chenopodium album* Linn. *Proc. Ind. Acad. Sci., B.*4 : 179–200.

Billings, F. H., 1934.—Male gametophyte of *Atriplex hymenelytra*. *Bot. Gaz.*, 95 : 477–484.

Bisulputra, T., 1960.—Anatomical and morphological studies in the Chenopodiaceae. I. Inflorescence of *Atriplex* and *Bassia*. *Aust. J. Bot.*, 8 : 226–242.

Black, J. M., 1948.—" Flora of South Australia ". Part II.

Cole, J. F., 1895.—Polyembryony. *Nature*, 51 : 558.

Favorsky, N., 1928.—Materialien sur biologie und embryologie der suckerrube. *Trudy Nsuch. Inst. Selek*, 2 : 1–18.

Johansen, D. A., 1950.—" Plant Embryology ". (Chronica Botanica Co. Walthon, Mass.).

Mahabale, T. S., and Solanky, I. N., 1953*a*.—Studies in the Chenopodiaceae. I. Embryology of *Suaeda fruticosa* Forsk. *Jour. Univ. Bombay*, 21 (5) : 81–92.

———, ———, 1953*b*.—Studies in the Chenopodiaceae. III. Embryology of *Kochia scoparia* Schard. *Jour. Univ. Bombay*, 22 (3) : 18–25.

———, ———, 1954*a*.—Studies in the Chenopodiaceae. II. Embryology of *Arthrocnemum indicum* Moq. *Proc. Ind. Acad. Sci.*, 39B : 212–222.

———, ———, 1954*b*.—Studies in the Chenopodiaceae. IV. Embryology of *Chenopodium ambrosioides* Linn. *Jour. Univ. Bombay*, 22 (5) : 31–42.

———, ———, 1954*c*.—Studies in the Chenopodiaceae. V. Embryology of *Chenopodium murale* Linn. *Jour. Univ. Bombay*, 23 (3) : 25–37.

Miller, H. A., Kline, H. J., and Weber, A. V., 1959.—The development of the androecium, the gynoecium, and the embryo of *Chenopodium ambrosioides* L. 9th Cong. Internat. Bot., 2 : 263–264.

Soueges, R., 1920.—Development de l'embryon chez le *Chenopodium bonus-henricus* L. *C. R. Acad. Sci. Paris*, 170 : 467–469. (Quoted in Johansen).

Woodland, Poh S., 1964.—The floral morphology and embryology of *Themeda australis* (R. Br.) Stapf. *Aust. Jour. Bot.*, 12 : 157–172.